Supporting Information

The First Ln−MOF as a Trifunctional Luminescent Probe for Efficient Sensing of aspartic acid, Fe^{3+} and DMSO

Dong-Dong Yang[a], Li-Ping Lu*[a], Si-Si Feng[ab], Miao-Li Zhu*[ab]

[a]Institute of Molecular Science, Key Laboratory of Chemical Biology and Molecular Engineering of the Education Ministry, Shanxi University, Taiyuan, Shanxi 030006, People' s Republic of China. luliping@sxu.edu.cn.

[b]Key Laboratory of Materials for Energy Conversion and Storage of Shanxi Province; Shanxi University, Taiyuan, Shanxi 030006, People's Republic of China. miaoli@sxu.edu.cn

Corresponding Author
*E-mail: luliping@sxu.edu.cn
*E-mail: miaoli@sxu.edu.cn

Table of Contents

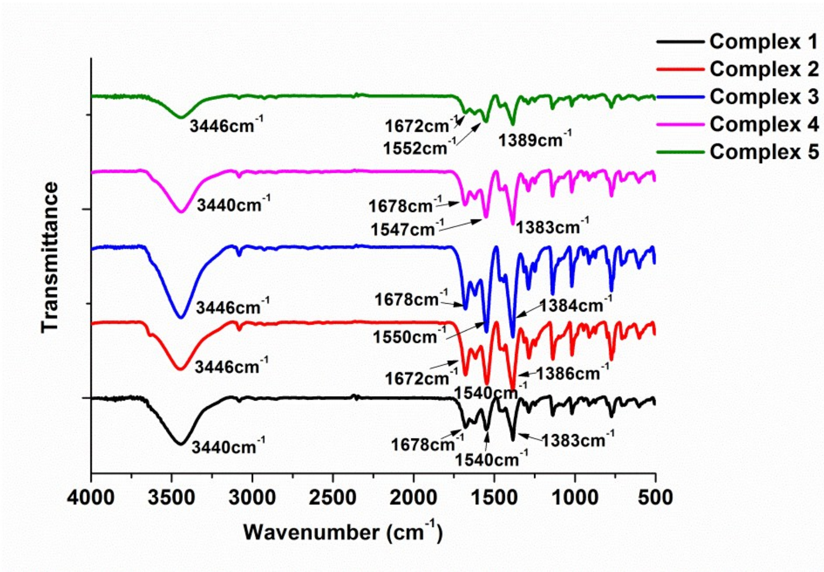

Fig. S1 IR spectra of complexes **1–5** (KBr, cm^{-1}).

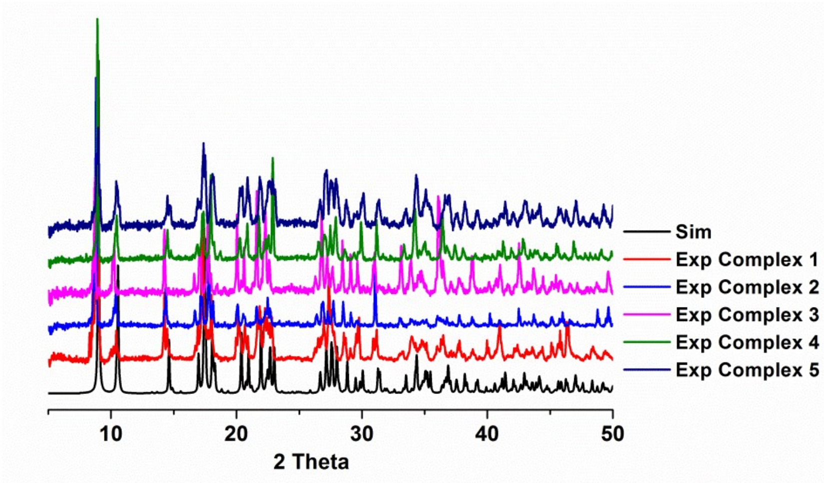

Fig. S2 PXRD patterns of complexes **1** - **5** in the 2θ range of 5 to 50°, showed the high phase purity of the complexes.

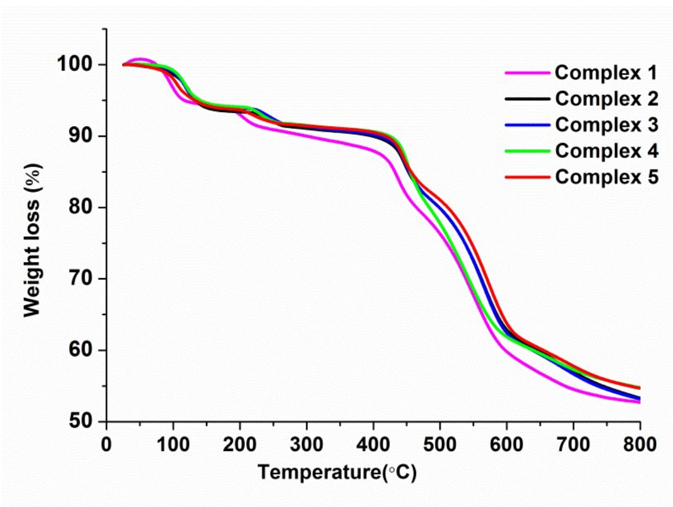

Fig. S3 The thermal curves of complex **1**–**5**, indicated their good stabilities in the range of RT-400 °C.

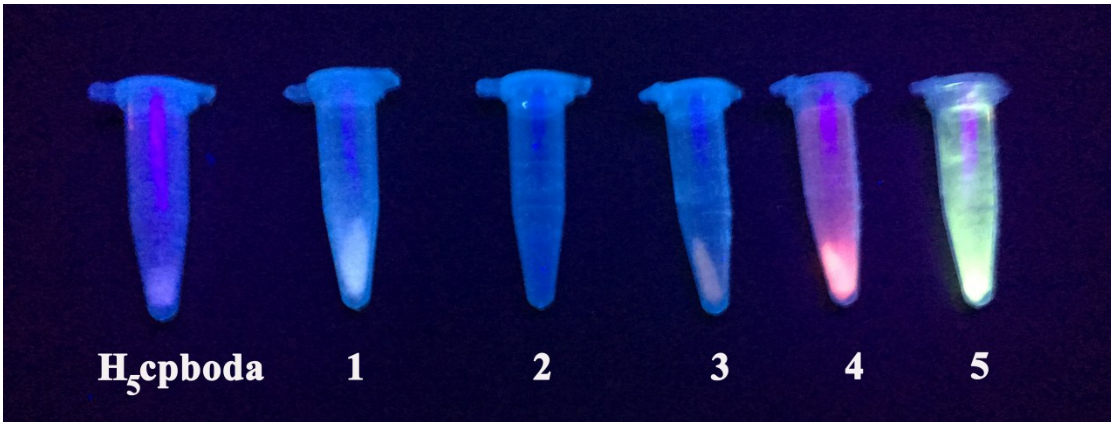

Fig. S4 Digital photograph of all complexes **1** – **5** under irradiation of UV light (254 nm)

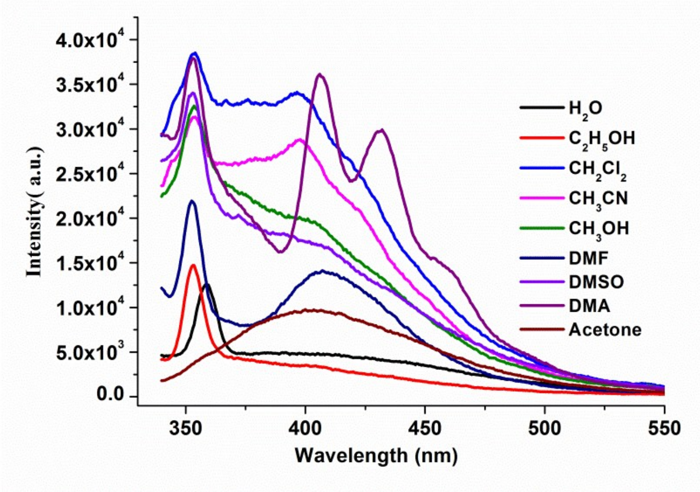

Fig. S5 Luminescence spectra for **1** dispersed in various organic solvents (5 mL, 2 mg **1**).

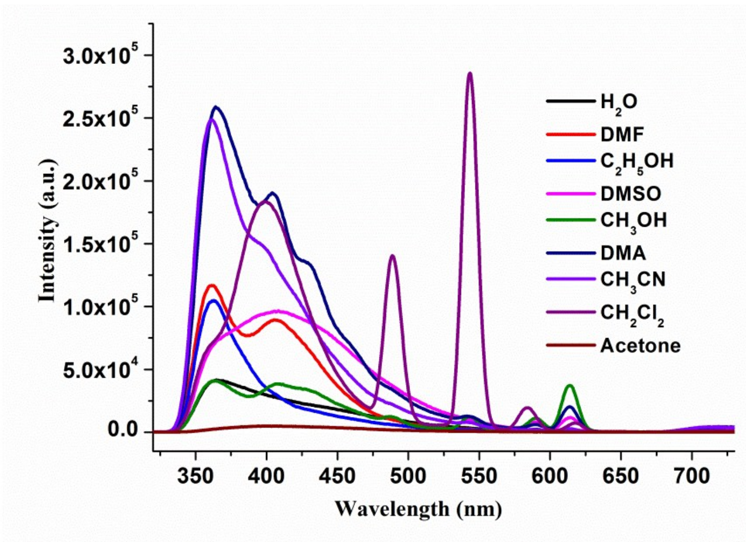

Fig. S6 Luminescence spectra for **4** dispersed in various organic solvents (5 mL, 2 mg **4**).

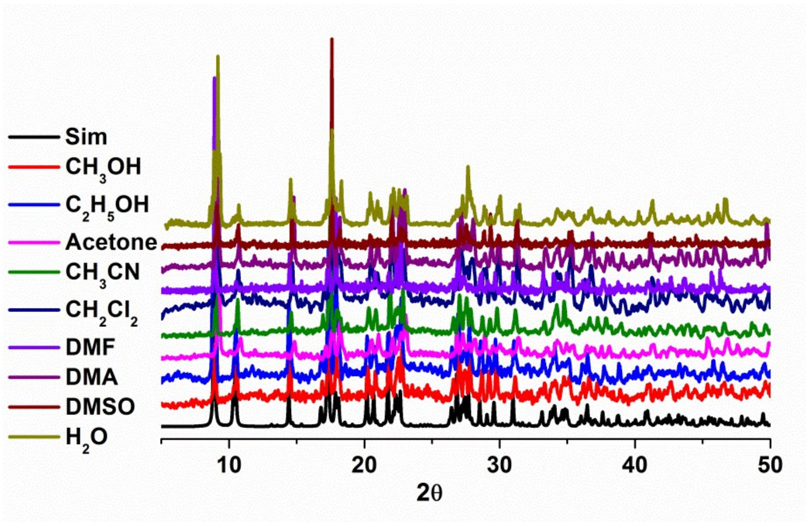

Fig S7. The PXRD patterns of complex **5** after immersing in different organic solvents for 24h.

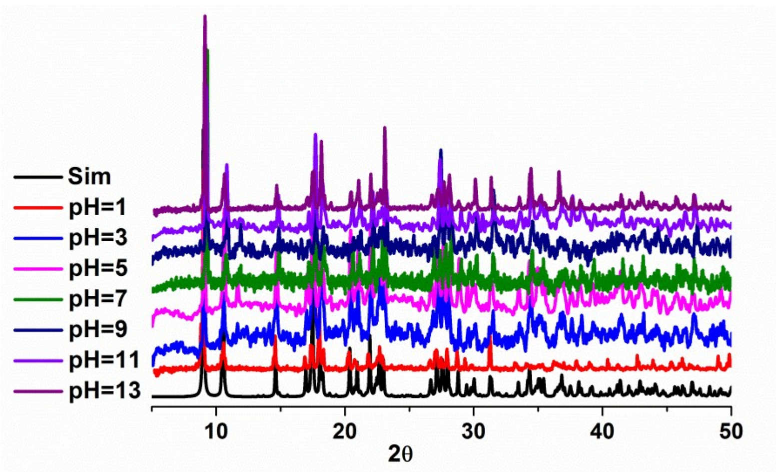

Fig S8. The PXRD patterns of complex **5** after immersing in aqueous solution with different pH for 24h.

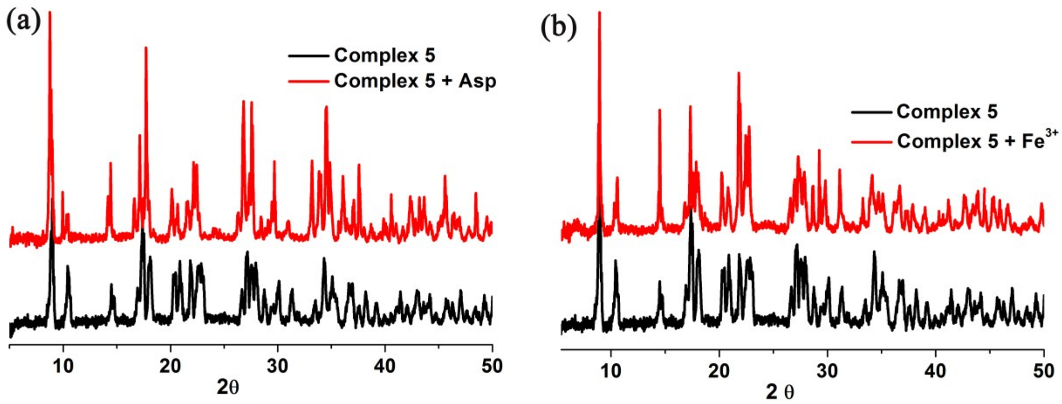

Fig. S9. The PXRD patterns of **5** and the recognition of aspartic acid (a) and Fe^{3+} (b) after five recycling processes.

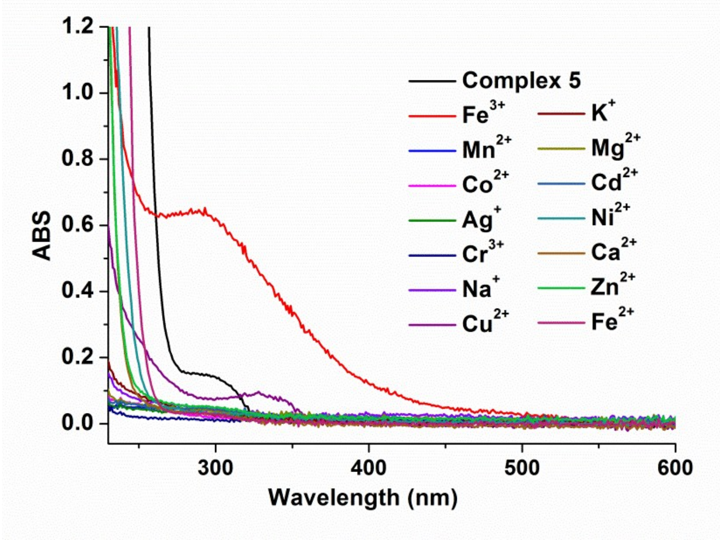

Fig S10 UV−vis absorption of aqueous solution containing complex **5** and Fe^{3+}, indicated that the fluorescence quenching mechanism is not caused by the excitation or emission spectra of the compounds overlapped.

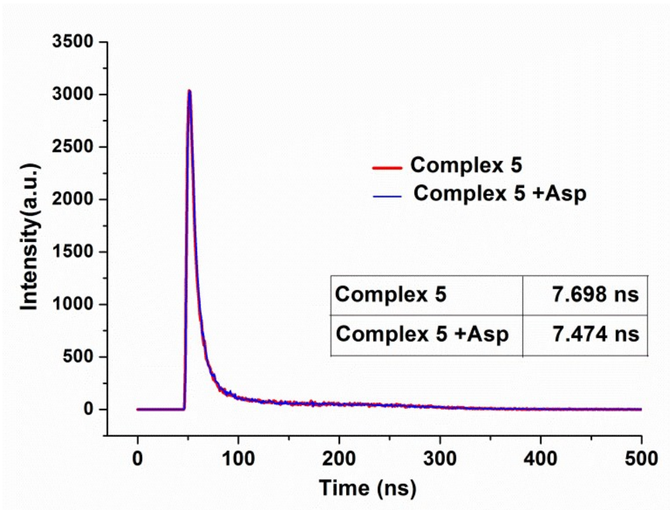

Fig. S11 The luminescence decay lifetimes of the complexes **5** and aspartic acid treated materials.

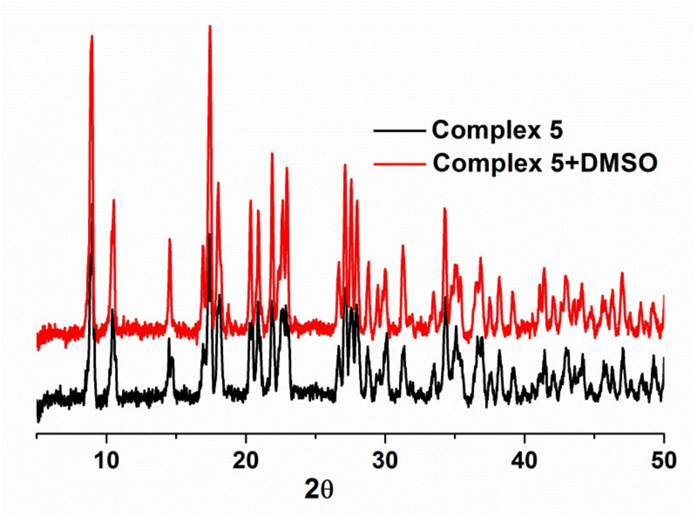

Fig. S12. The PXRD patterns of **5** and the recognition of DMSO after soaking.

Tables S1-1. Selected bond lengths [Å] and angles [°] for complex **1**

La1—O10^{i}	2.424 (3)	La1—O9^{iv}	2.509 (3)
La1—O7^{ii}	2.432 (3)	La1—O4^{v}	2.546 (3)
La1—O2	2.480 (3)	La1—O13	2.554 (3)
La1—O6^{iii}	2.494 (3)	La1—O14	2.620 (3)
O10^{i}—La1—O7^{ii}	147.81 (10)	O9^{iv}—La1—O4^{v}	139.90 (9)
O10^{i}—La1—O2	94.89 (9)	O10^{i}—La1—O13	74.30 (9)
O7^{ii}—La1—O2	72.79 (9)	O7^{ii}—La1—O13	133.78 (9)
O10^{i}—La1—O6^{iii}	94.88 (9)	O2—La1—O13	139.67 (9)
O7^{ii}—La1—O6^{iii}	82.99 (9)	O6^{iii}—La1—O13	72.17 (9)
O2—La1—O6^{iii}	148.15 (9)	O9^{iv}—La1—O13	69.07 (10)
O10^{i}—La1—O9^{iv}	83.97 (10)	O4^{v}—La1—O13	131.90 (9)
O7^{ii}—La1—O9^{iv}	117.86 (10)	O10^{i}—La1—O14	144.10 (10)
O2—La1—O9^{iv}	71.23 (10)	O7^{ii}—La1—O14	66.53 (10)
O6^{iii}—La1—O9^{iv}	140.02 (9)	O2—La1—O14	111.46 (10)
O10^{i}—La1—O4^{v}	73.60 (9)	O6^{iii}—La1—O14	75.69 (10)
O7^{ii}—La1—O4^{v}	74.75 (10)	O9^{iv}—La1—O14	82.12 (10)
O2—La1—O4^{v}	77.95 (9)	O4^{v}—La1—O14	134.03 (10)
O6^{iii}—La1—O4^{v}	75.92 (9)	O13—La1—O14	69.82 (10)

Symmetry codes: (i) -*x*+1/2, *y*-1/2, -*z*+1/2; (ii) *x*+1, *y*, *z*; (iii) -*x*+1, -*y*, -*z*; (iv) *x*+1/2, -*y*+1/2, *z*-1/2.

Tables S1-2. Selected bond lengths [Å] and angles [°] for complex **2**

Nd1—O2^{i}	2.366 (3)	Nd1—O1	2.475 (3)
Nd1—O6^{ii}	2.392 (3)	Nd1—O9^{v}	2.488 (3)
Nd1—O11^{iii}	2.427 (3)	Nd1—O14	2.497 (3)
Nd1—O7^{iv}	2.443 (3)	Nd1—O13	2.555 (4)
O2^{i}—Nd1—O6^{ii}	147.63 (12)	O1—Nd1—O9^{v}	139.51 (12)
O2^{i}—Nd1—O11^{iii}	94.36 (12)	O2^{i}—Nd1—O14	73.80 (12)
O6^{ii}—Nd1—O11^{iii}	72.95 (12)	O6^{ii}—Nd1—O14	134.77 (12)
O2^{i}—Nd1—O7^{iv}	96.10 (12)	O11^{iii}—Nd1—O14	138.70 (12)
O6^{ii}—Nd1—O7^{iv}	82.85 (12)	O7^{iv}—Nd1—O14	72.21 (11)
O11^{iii}—Nd1—O7^{iv}	149.09 (12)	O1—Nd1—O14	69.13 (12)
O2^{i}—Nd1—O1	82.68 (11)	O9^{v}—Nd1—O14	131.13 (12)
O6^{ii}—Nd1—O1	118.44 (12)	O2^{i}—Nd1—O13	144.05 (12)
O11^{iii}—Nd1—O1	70.19 (12)	O6^{ii}—Nd1—O13	67.42 (13)
O7^{iv}—Nd1—O1	140.04 (12)	O11^{iii}—Nd1—O13	109.68 (12)
O2^{i}—Nd1—O9^{v}	73.75 (11)	O7^{iv}—Nd1—O13	77.00 (12)
O6^{ii}—Nd1—O9^{v}	74.63 (12)	O1—Nd1—O13	81.00 (13)
O11^{iii}—Nd1—O9^{v}	79.17 (12)	O9^{v}—Nd1—O13	135.50 (12)
O7^{iv}—Nd1—O9^{v}	76.03 (11)	O14—Nd1—O13	70.49 (12)

Symmetry codes: (i) -*x*+1, -*y*, -*z*+1; (ii) *x*+1/2, -*y*+1/2, *z*+1/2; (iii) *x*-1/2, -*y*+1/2, *z*+1/2; (iv) -*x*+3/2, *y*-1/2, -*z*+1/2; (v) -*x*+2, -*y*, -*z*+1。

Tables S1-3. Selected bond lengths [Å] and angles [°] for complex **3**

Sm1—O2^{i}	2.342 (3)	Sm1—O1	2.449 (3)
Sm1—O6^{ii}	2.362 (3)	Sm1—O9^{v}	2.460 (3)
Sm1—O11^{iii}	2.408 (3)	Sm1—O14	2.479 (3)
Sm1—O7^{iv}	2.410 (3)	Sm1—O13	2.514 (3)
O2^{i}—Sm1—O6^{ii}	147.27 (10)	O1—Sm1—O9^{v}	139.61 (10)
O2^{i}—Sm1—O11^{iii}	94.40 (10)	O2^{i}—Sm1—O14	73.63 (9)
O6^{ii}—Sm1—O11^{iii}	72.69 (10)	O6^{ii}—Sm1—O14	135.33 (10)
O2^{i}—Sm1—O7^{iv}	96.95 (9)	O11^{iii}—Sm1—O14	138.58 (10)
O6^{ii}—Sm1—O7^{iv}	82.54 (10)	O7^{iv}—Sm1—O14	72.13 (10)
O11^{iii}—Sm1—O7^{iv}	149.29 (10)	O1—Sm1—O14	69.17 (10)

O2^{i}—Sm1—O1	82.21 (10)	O9^{v}—Sm1—O14	130.83 (9)
O6^{ii}—Sm1—O1	118.86 (10)	O2^{i}—Sm1—O13	144.30 (10)
O11^{iii}—Sm1—O1	69.99 (10)	O6^{ii}—Sm1—O13	67.74 (10)
O7^{iv}—Sm1—O1	139.85 (10)	O11^{iii}—Sm1—O13	108.56 (10)
O2^{i}—Sm1—O9^{v}	74.00 (9)	O7^{iv}—Sm1—O13	77.21 (11)
O6^{ii}—Sm1—O9^{v}	74.13 (10)	O1—Sm1—O13	80.60 (10)
O11^{iii}—Sm1—O9^{v}	79.69 (9)	O9^{v}—Sm1—O13	135.67 (10)
O7^{iv}—Sm1—O9^{v}	76.21 (10)	O14—Sm1—O13	71.06 (10)

Symmetry codes: (i) -*x*+1, -*y*, -*z*+1; (ii) *x*+1/2, -*y*+1/2, *z*+1/2; (iii) *x*-1/2, -*y*+1/2, *z*+1/2; (iv) -*x*+3/2, *y*-1/2, -*z*+1/2; (v) -*x*+2, -*y*, -*z*+1.

Tables S2-4. Selected bond lengths [Å] and angles [°] for complex **4**

Eu1—O2^{i}	2.312 (3)	Eu1—O9^{v}	2.432 (3)
Eu1—O6^{ii}	2.342 (3)	Eu1—O1	2.434 (3)
Eu1—O11^{iii}	2.381 (3)	Eu1—O14	2.441 (3)
Eu1—O7^{iv}	2.388 (3)	Eu1—O13	2.484 (3)
O2^{i}—Eu1—O6^{ii}	147.16 (10)	O9^{v}—Eu1—O1	139.36 (10)
O2^{i}—Eu1—O11^{iii}	94.09 (10)	O2^{i}—Eu1—O14	73.52 (10)
O6^{ii}—Eu1—O11^{iii}	72.99 (10)	O6^{ii}—Eu1—O14	135.44 (10)
O2^{i}—Eu1—O7^{iv}	97.51 (10)	O11^{iii}—Eu1—O14	138.54 (10)
O6^{ii}—Eu1—O7^{iv}	82.32 (10)	O7^{iv}—Eu1—O14	71.70 (10)
O11^{iii}—Eu1—O7^{iv}	149.75 (10)	O9^{v}—Eu1—O14	130.33 (10)
O2^{i}—Eu1—O9^{v}	74.18 (10)	O1—Eu1—O14	69.46 (10)
O6^{ii}—Eu1—O9^{v}	73.91 (10)	O2^{i}—Eu1—O13	144.15 (11)
O11^{iii}—Eu1—O9^{v}	80.19 (10)	O6^{ii}—Eu1—O13	68.18 (11)
O7^{iv}—Eu1—O9^{v}	76.30 (10)	O11^{iii}—Eu1—O13	107.83 (11)
O2^{i}—Eu1—O1	81.35 (10)	O7^{iv}—Eu1—O13	77.75 (11)
O6^{ii}—Eu1—O1	119.55 (10)	O9^{v}—Eu1—O13	136.25 (10)
O11^{iii}—Eu1—O1	69.61 (10)	O1—Eu1—O13	80.30 (10)
O7^{iv}—Eu1—O1	139.77 (10)	O14—Eu1—O13	71.26 (10)

Symmetry codes: (i) -*x*+1, -*y*, -*z*+1; (ii) *x*+1/2, -*y*+1/2, *z*+1/2; (iii) *x*-1/2, -*y*+1/2, *z*+1/2; (iv) -*x*+3/2, *y*-1/2, -*z*+1/2; (v) -*x*+2, -*y*, -*z*+1.

Tables S1-5. Selected bond lengths [Å] and angles [°] for complex **5**

Tb1—O2^{i}	2.302 (4)	Tb1—O9^{v}	2.422 (4)
Tb1—O6^{ii}	2.331 (4)	Tb1—O1	2.426 (4)
Tb1—O2^{i}	2.302 (4)	Tb1—O9^{v}	2.421 (3)
Tb1—O6^{ii}	2.330 (3)	Tb1—O1	2.425 (4)
Tb1—O11^{iii}	2.371 (3)	Tb1—O14	2.438 (4)
Tb1—O7^{iv}	2.375 (3)	Tb1—O13	2.468 (4)
O2^{i}—Tb1—O6^{ii}	147.17 (13)	O11^{iii}—Tb1—O1	69.43 (13)
O2^{i}—Tb1—O11^{iii}	94.04 (13)	O7^{iv}—Tb1—O1	139.57 (13)
O6^{ii}—Tb1—O11^{iii}	72.79 (12)	O11^{iii}—Tb1—O1	69.43 (13)
O2^{i}—Tb1—O7^{iv}	97.90 (12)	O7^{iv}—Tb1—O1	139.57 (13)
O6^{ii}—Tb1—O7^{iv}	82.49 (12)	O9^{v}—Tb1—O1	139.48 (12)
O11^{iii}—Tb1—O7^{iv}	150.01 (13)	O2^{i}—Tb1—O14	73.56 (12)
O2^{i}—Tb1—O9^{v}	74.28 (13)	O6^{ii}—Tb1—O14	135.67 (12)
O6^{ii}—Tb1—O9^{v}	73.93 (13)	O11^{iii}—Tb1—O14	138.17 (13)
O11^{iii}—Tb1—O9^{v}	80.51 (12)	O7^{iv}—Tb1—O14	71.79 (12)
O7^{iv}—Tb1—O9^{v}	76.46 (12)	O9^{v}—Tb1—O14	130.43 (12)
O2^{i}—Tb1—O1	81.22 (13)	O1—Tb1—O14	69.24 (13)
O6^{ii}—Tb1—O1	119.36 (13)	O2^{i}—Tb1—O13	144.36 (13)
O7^{iv}—Tb1—O13	78.09 (14)	O1—Tb1—O13	79.86 (13)
O9^{v}—Tb1—O13	136.41 (13)	O14—Tb1—O13	71.57 (13)

Symmetry codes: (i) -*x*+1, -*y*, -*z*+1; (ii) *x*+1/2, -*y*+1/2, *z*+1/2; (iii) *x*-1/2, -*y*+1/2, *z*+1/2; (iv) -*x*+3/2, *y*-1/2, -*z*+1/2; (v) -*x*+2, -*y*, -*z*+1.

Table S2 Comparison of various MOFs sensors for the detection of aspartic acid.

MOFs and related materials	Analyte	K_{sv} (M^{-1})	Detection Limit (mol/L)	Ref
Ag + @Eu-complex	aspartic acid	-	4.6×10^{-7}	S1
Ce–BBAS	aspartic acid	-	2.6×10^{-7}	S2
Cu/Tb@Zn-MOF	aspartic acid	-	4.132×10^{-6}	S3
$[[Tb(\mu_6\text{-}H_2cpboda)(\mu_2\text{-}OH_2)_2]\cdot H_2O]_n$	aspartic acid	9.80×10^{3}	7.95×10^{-6}	This work
$\{[Eu(L)(H_2O)_2]\cdot DMF\}_n$	aspartic acid	1.09×10^{3}	5.91×10^{-5}	S4

References:

S1. H. Weng, B. Yan, *Sens. Actuator B,* 2017, **253**, 1006–1011.

S2. P. Y. Wu, M. Jiang, X. F. Hu, J.R. Wang, G. J. He, Y. Shi, Y. Li, W. Liu and J. Wang, *RSC Adv*., 2016, **6**, 27944–27951.

S3. G.F. Ji , T. X. Zheng, X.C. Gao, Z. L. Liu, *Sens. Actuator B,* 2019, **284**, 91–95.

S4. A. F. Yang, S. L. Hou, Y. Shi, G. L. Yang, D. B. Qin and B. Zhao, *Inorg.Chem*., 2019, **58**, 6356-6362.